Direct observation of Landau-Zener tunneling in a curved optical waveguide coupler

F. Dreisow,[1,*] A. Szameit,[1] M. Heinrich,[1] S. Nolte,[1,2] and A. Tünnermann[1,2]
[1]*Institute of Applied Physics, Friedrich-Schiller-University Jena, Max-Wien-Platz 1, 07743 Jena, Germany*
[2]*Fraunhofer Institute for Applied Optics and Precision Engineering, Albert-Einstein-Strasse 7, 07745 Jena, Germany*

M. Ornigotti and S. Longhi
Dipartimento di Fisica and Istituto di Fotonica e Nanotecnologie del Consiglio Nazionale delle Ricerche, Politecnico di Milano, Piazza L da Vinci 32, I-20133 Milan, Italy
(Received 9 February 2009; published 5 May 2009)

An electromagnetic realization of Landau-Zener (LZ) tunneling is experimentally demonstrated in femtosecond-laser written waveguide couplers with a cubically bent axis. Quantitative measurements of light evolution inside the coupler, based on fluorescence imaging, enable to trace the detailed dynamics of the LZ process. The experimental results are in good agreement with the theoretical LZ model for linear crossing of energy levels with constant coupling of finite duration.

DOI: 10.1103/PhysRevA.79.055802 PACS number(s): 42.82.Et, 03.65.Xp, 33.80.Be

First introduced by Landau in the context of atomic scattering processes [1] and by Zener in the study of the electronic properties of a biatomic molecule [2], the Landau-Zener (LZ) transition represents a fundamental dynamical process which occurs at the intersection of two energy levels that repel each other. Owing to its general character, the LZ model is encountered in different physical fields and systems. Among others, LZ transitions have been investigated for Rydberg atoms [3], molecular nanomagnets [4,5], cold atoms and Bose-Einstein condensates in accelerated optical lattices [6,7], field-driven superlattices [8], current-driven Josephson junctions [9], and Cooper-pair box qubits [10]. Classical analogs of LZ transitions have been also investigated, including polarization rotation in an optical cavity [11] and LZ tunneling of light waves in coupled waveguides [12,13]. Many extensions of the original LZ model have been studied in the past few years as well, including the effect of different temporal interaction profiles [14], nonlinearities [15], finite-coupling duration effects [16], multistate dynamics [17,18], decoherence, noise and dissipation [19,20], to name a few. In spite of the vast literature on LZ models, direct observations of time-resolved evolution of level occupancy during LZ transition are very few, and mainly reported for light polarization dynamics in classical optical cavities [11]. Coupled optical waveguides, on the other hand, have been recently shown to provide an accessible laboratory system to mimic, at a classical level, the coherent control of quantum mechanical tunneling [21,22]. In such structures, the fast temporal evolution of the quantum mechanical wave function is replaced by spatial light propagation along the waveguides, and occupancy probabilities in the two wells can be measured by tracing the flow of light using fluorescence imaging or scanning optical microscopy techniques.

In this Brief Report we present spatially resolved measurements of LZ tunneling dynamics for light waves in cubically curved coupled waveguides fabricated with the femtosecond-laser writing technique, which provides an optical realization of the LZ model with linear energy level crossing and with constant coupling of finite duration [13].

We consider the propagation of a monochromatic wave at the wavelength $\lambda = 2\pi/k$ in an optical directional coupler of length L made of two identical single-mode waveguides separated by the distance d in the transverse x direction. The propagation axis of the coupler is assumed to be weakly curved along the paraxial propagation direction z [Fig. 1(a)]. To mimic LZ tunneling with linear crossing of energy levels, a cubically bent profile $x_0(z)$ for the waveguide axis is assumed according to [13]

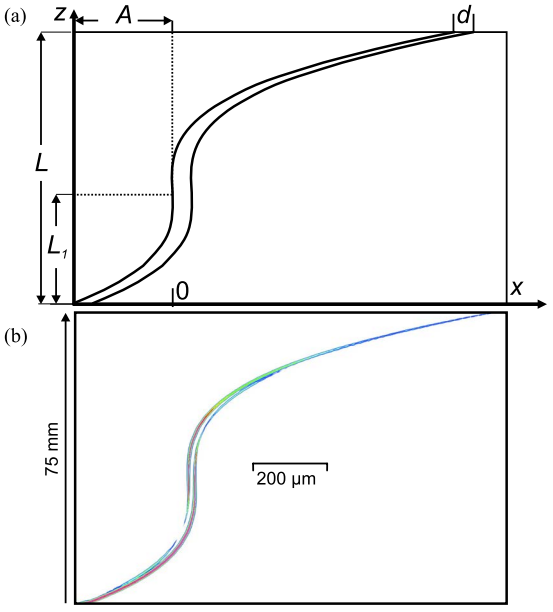

FIG. 1. (Color online) (a) Schematic of a cubically curved directional coupler for the observation of LZ dynamics. (b) Fluorescence measurement of curved directional coupler with spacing $d = 17$ μm and cubic profile $A = 300$ μm, $L_1 = 31.25$ mm, (the arrow indicates the propagation direction).

*f.dreisow@uni-jena.de

$$x_0(z) = \frac{A}{L_1^3}(z - L_1)^3, \tag{1}$$

$(0 < z < L)$, where $A (A \ll L)$ is the full lateral shift of the waveguides between input $(z=0)$ and zero curvature $(z=L_1)$ planes and L_1 is the offset position at which the axis curvature $\ddot{x}_0(z)$ vanishes. Under the scalar and paraxial approximations, the electric field amplitude can be written as $E(x,y,z,t) = \psi(x,y,z)\exp[i(kn_s z - \omega t)] + \text{c.c.}$, where n_s is the refractive index of the substrate, $\omega = kc_0$ and $\psi(x,y,z)$ is the slow-varying field envelope $(|\partial^2\psi/\partial z^2| \ll k|\partial\psi/\partial z|)$ which satisfies the paraxial wave equation,

$$i\lambda\frac{\partial\psi}{\partial z} = -\frac{\lambda^2}{2n_s}\nabla_{x,y}^2\psi + V[x - x_0(z), y]\psi. \tag{2}$$

In Eq. (2), $\lambda \equiv \lambda/2\pi = 1/k$ is the reduced wavelength and $V(x,y) \equiv [n_s^2 - n^2(x,y)]/(2n_s) \simeq n_s - n(x,y)$, $n(x,y)$ is the double-well refractive index profile of the coupler. Light propagation in the curved coupler is at best captured in the waveguide reference frame $x' = x - x_0(z)$, and $z' = z - L_1$, where the waveguides appear to be straight and a fictitious transverse index gradient proportional to the local curvature $\ddot{x}_0(z)$ appears (see, e.g., [21]). In the tight-binding approximation, the amplitudes $a_1(z')$ and $a_2(z')$ of light waves trapped in the two waveguides are readily obtained from Eq. (2) and read as [13]

$$i\frac{d}{dz'}\begin{pmatrix} a_1 \\ a_2 \end{pmatrix} = \begin{pmatrix} \eta^2 z' & \Omega_0 \\ \Omega_0 & -\eta^2 z' \end{pmatrix}\begin{pmatrix} a_1 \\ a_2 \end{pmatrix}, \tag{3}$$

$(-L_1 < z' < L - L_1)$, where Ω_0 is the coupling rate between the two waveguides of the coupler and η^2 is given by [13]

$$\eta^2 = \frac{3dAn_s}{\lambda L_1^3}. \tag{4}$$

In their present form, Eq. (3) describe LZ tunneling with linear crossing of energy level, at a rate η^2 given by Eq. (4), and with constant coupling Ω_0 of finite duration L. The solution to Eq. (3) can be expressed in terms of the parabolic cylinder function $D_\nu(z')$ according to (see Ref. [16] for details)

$$a_1(z') = aD_\nu(\sqrt{2}\eta z' e^{-i\pi/4}) + bD_\nu(\sqrt{2}\eta z' e^{i3\pi/4}), \tag{5}$$

$$a_2(z') = \frac{\Omega_0}{\eta\sqrt{2}}e^{-i\pi/4}[-aD_{\nu-1}(\sqrt{2}\eta z' e^{-i\pi/4}) + bD_{\nu-1}(-\sqrt{2}\eta z' e^{-i\pi/4})], \tag{6}$$

where we have set $\nu = i\Omega_0^2/2\eta^2$. The constants a and b entering in Eqs. (5) and (6) have to be determined once the initial conditions $a_1(-L_1)$ and $a_2(-L_1)$ are assigned.

For the experimental verification of the LZ dynamics [Eqs. (5) and (6)], a set of cubically curved waveguide couplers were manufactured by fs laser microstructuring [23]. Thereby an ultrashort laser pulse is focused with a 20× microscope objective that has a numerical aperture of 0.35 inside fused silica. By moving the sample transversally to the laser beam [Fig. 2(a)] micromodifications along almost arbitrary curves can be formed. The writing parameters of the

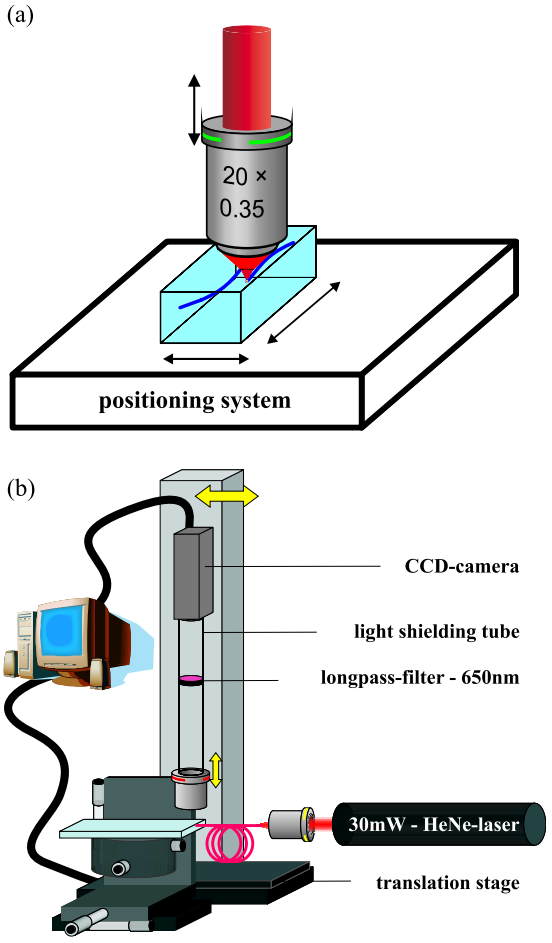

FIG. 2. (Color online) Schematic setups for (a) waveguide manufacturing and (b) fluorescence measurements.

Ti:sapphire amplifier system operating at a wavelength of 800 nm and a repetition rate of 100 kHz were tuned to 28 mW average power, 170 fs pulse length and 120 mm/min scanning velocity. These parameters yield a refractive index increase of $\Delta n \approx 6 \cdot 10^{-4}$, and low loss wave guiding of the fundamental mode for a wavelength $\lambda = 633$ nm is supported [24]. Using fused silica glass with a high content of silanol (Hereaus Suprasil 311) leads to massive formation of nonbridging oxygen-hole color centers. When excited with a HeNe laser ($\lambda = 633$ nm), these color centers emit fluorescence light around 650 nm [25], which can be conveniently detected from the top of the sample [see Fig. 2(b)]. This technique enables to accurately map the flow of light along the sample as discussed in detail in Ref. [26]. The corresponding fluorescence image is depicted in Fig. 1(b). Since the curved coupler shows a lateral shift of 1.82 mm from input to output planes, the complete fluorescence image of Fig. 1(b) was obtained by stitching together five single images, which are laterally shifted in the x direction by 450 μm each from the next. To make a quantitative analysis of light evolution along the two curved waveguides, a coordinate transformation $x' = x - x_0(z)$ and $z' = z - L_1$ to the waveguide reference frame was digitally applied to these images. Further, a fine adjustment was made to align the maxima of the fields in one column, which results in images of straight

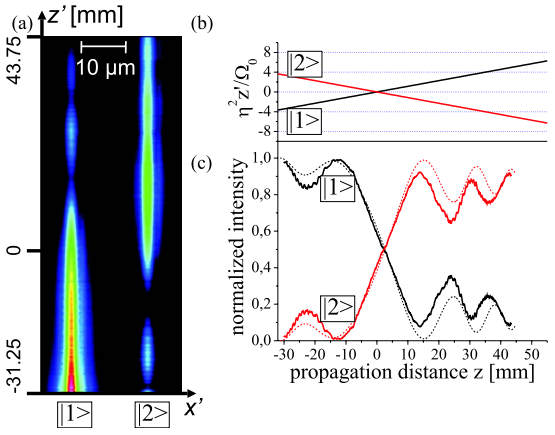

FIG. 3. (Color online) Experimental observation of the Landau-Zener tunneling process. The separation of the waveguides is $d=17$ μm resulting in a coupling rate $\Omega_0=0.063$ mm^{-1}, the full bending amplitude is $A=300$ μm and the bending length is $L_1=31.25$ mm. (a) Digitally straightened fluorescence image, (b) detuning $\eta^2 z'/\Omega_0$ of the waveguides due to the curvature normalized to the coupling constant Ω_0 and (c) measured (solid) and theoretical (dashed) intensities $|a_1(z')|^2$ and $|a_2(z')|^2$ in the two waveguides plotted vs propagation distance in the reference frame z'. State $|1\rangle$ was excited initially.

guides. Their longitudinal-to-transverse aspect ratio can be additionally enlarged, which allows for a clear visualization and simple analysis of the data [see Figs. 3(a) and 4(a)]. The power trapped in the waveguides is gained by maximum filtering the image fractions containing the respective waveguide. The intrinsic propagation losses of ≈ 0.4 dB/cm and the radiation losses due to waveguide bending are removed by normalization to the total power. Hence, the intensities $|a_1(z')|^2$ and $|a_2(z')|^2$ can be plotted versus propagation distance z' and compared with the theoretical curves as given by Eqs. (5) and (6). The coupling rates Ω_0 have been simply obtained by measurements of coupling lengths in pairs of

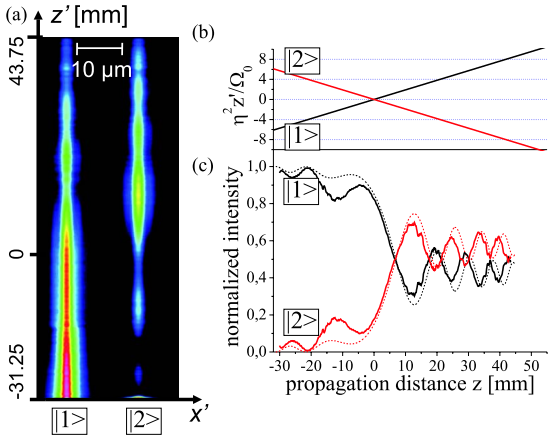

FIG. 4. (Color online) Same as Fig. 3 but for a full bending amplitude of $A=500$ μm resulting in incomplete power transfer to an average level of $\approx 50\%$.

straight waveguides, fabricated together with the curved ones.

Experimentally the excitation is accomplished by fiber butt coupling, which satisfies the initial conditions $a_1(-L_1)=1$ and $a_2(-L_1)=0$. In a first instance we demonstrate a slow transition with a small full bending amplitude $A=300$ μm and offset position $L_1=31.25$ mm, which corresponds to the adiabatic regime. The appropriate fluorescence measurement is depicted in Fig. 3(a), and the experimental and theoretical intensities $|a_1(z')|^2$ and $|a_2(z')|^2$ are compared in Fig. 3(c). The graph in Fig. 3(b) shows the z'-dependent detuning of the two level system and its smooth fading into the resonance. In a region around this resonance ($z' \approx -11$ mm to $+11$ mm) an interaction of the states becomes possible and due to the large ratio of Ω_0^2/η^2 a power exchange is achieved. To transfer the power efficiently and enduringly to $|2\rangle$, the resonance must be constrained again. Figure 3 depicts that this condition is well achieved for a full lateral shift of $A=300$ μm and waveguide spacing $d=17$ μm, which corresponds to an interaction coefficient $\Omega_0=0.063$ mm^{-1}. At $z' \geq 11$ mm more than 90% of the power is trapped in the second state. An oscillation with slowly decaying amplitude and growing frequency sets in, where the explicit behavior depends strongly on the parameters Ω_0 and η.

Additionally, an incomplete power transfer regime is shown in Fig. 4. Here, the full bending amplitude is $A=500$ μm resulting in a larger value for η. Therefore, the transition becomes nearly diabatic and the system can evolve faster. Due to the curvature the two states are out of phase at the first section of the sample ($z'=-L_1$ to -10 mm) [see Fig. 4(c)] and the power exchange is basically suppressed. The dephasing gradient is strong with respect to the interaction frequency Ω_0 [Fig. 4(b)], which yields a narrow resonance around $z'=0$. Around the resonance the states $|1\rangle$ and $|2\rangle$ can exchange power, but the oscillation period is too long to achieve a complete transfer. In the case of a full bending amplitude of $A=500$ μm (Fig. 4) the total power transfer rate is already decreased to approximately 50%. A further enlarging of the detuning gradient would result in a fully diabatic behavior, where the occupation probability cannot evolve and the states cannot follow the evolution of the system.

In conclusion, we reported on the visualization of light dynamics in an optical directional coupler fabricated with the femtosecond-laser writing technique, which mimics the LZ tunneling process with a linear crossing of the energy levels and a finite-coupling duration. As compared to previous realizations of LZ models reported in other physical contexts, our experimental system provides a rather unique tool to accurately map the evolution of LZ tunneling. Extensions of this model, to investigate for instance nonlinear LZ tunneling in presence of Kerr nonlinearity, or decoherence effects in presence of waveguide imperfections, may be foreseen.

We acknowledge support by the Deutsche Forschungsgemeinschaft (Leibniz-Program and Research Unit 532 "Nonlinear spatio-temporal dynamics in dissipative and discrete optical systems").

[1] L. D. Landau, Phys. Z. Sowjetunion **1**, 89 (1932).
[2] C. Zener, Proc. R. Soc. London, Ser. A **137**, 696 (1932).
[3] J. R. Rubbmark, M. M. Kash, M. G. Littman, and D. Kleppner, Phys. Rev. A **23**, 3107 (1981).
[4] W. Wernsdorfer and R. Sessoli, Science **284**, 133 (1999); W. Wernsdorfer, R. Sessoli, A. Caneschi, D. Gatteschi, and A. Cornia, Europhys. Lett. **50**, 552 (2000).
[5] P. Foldi, M. G. Benedict, J. M. Pereira, and F. M. Peeters, Phys. Rev. B **75**, 104430 (2007).
[6] M. Jona-Lasinio, O. Morsch, M. Cristiani, N. Malossi, J. H. Müller, E. Courtade, M. Anderlini, and E. Arimondo, Phys. Rev. Lett. **91**, 230406 (2003).
[7] S. J. Woo, S. Choi, and N. P. Bigelow, Phys. Rev. A **72**, 021605(R) (2005).
[8] A. Sibille, J. F. Palmier, and F. Laruelle, Phys. Rev. Lett. **80**, 4506 (1998).
[9] K. Mullen, E. Ben-Jacob, and Z. Schuss, Phys. Rev. Lett. **60**, 1097 (1988).
[10] W. D. Oliver, Y. Yu, J. C. Lee, K. K. Berggren, L. S. Levitov, and T. P. Orlando, Science **310**, 1653 (2005); M. Sillanpaa, T. Lehtinen, A. Paila, Y. Makhlin, and P. Hakonen, Phys. Rev. Lett. **96**, 187002 (2006).
[11] R. J. C. Spreeuw, N. J. van Druten, M. W. Beijersbergen, E. R. Eliel, and J. P. Woerdman, Phys. Rev. Lett. **65**, 2642 (1990); D. Bouwmeester, N. H. Dekker, F. E. v. Dorsselaer, C. A. Schrama, P. M. Visser, and J. P. Woerdman, Phys. Rev. A **51**, 646 (1995).
[12] R. Khomeriki and S. Ruffo, Phys. Rev. Lett. **94**, 113904 (2005).
[13] S. Longhi, J. Opt. B: Quantum Semiclassical Opt. **7**, L9 (2005).
[14] F. T. Hioe and C. E. Carroll, Phys. Rev. A **32**, 1541 (1985).
[15] J. Liu, Libin Fu, Bi-Yiao Ou, Shin-Gang Chen, Dae-Il Choi, Biao Wu, and Qian Niu, Phys. Rev. A **66**, 023404 (2002).
[16] N. V. Vitanov and B. M. Garraway, Phys. Rev. A **53**, 4288 (1996).
[17] V. L. Pokrovsky and N. A. Sinitsyn, Phys. Rev. B **65**, 153105 (2002).
[18] M. V. Volkov and V. N. Ostrovsky, J. Phys. B **37**, 4069 (2004).
[19] E. Shimshoni and A. Stern, Phys. Rev. B **47**, 9523 (1993); K. Saito, M. Wubs, S. Kohler, Y. Kayanuma, and P. Hänggi, *ibid.* **75**, 214308 (2007).
[20] V. L. Pokrovsky and D. Sun, Phys. Rev. B **76**, 024310 (2007).
[21] G. Della Valle, M. Ornigotti, E. Cianci, V. Foglietti, P. Laporta, and S. Longhi, Phys. Rev. Lett. **98**, 263601 (2007).
[22] F. Dreisow, A. Szameit, M. Heinrich, T. Pertsch, S. Nolte, A. Tünnermann, and S. Longhi, Phys. Rev. Lett. **101**, 143602 (2008).
[23] K. Itoh, W. Watanabe, S. Nolte, and C. B. Schaffer, MRS Bull. **31**, 620 (2006).
[24] D. Blomer, A. Szameit, F. Dreisow, T. Schreiber, S. Nolte, and A. Tuennermann, Opt. Express **14**, 2151 (2006).
[25] A. Szameit, F. Dreisow, H. Hartung, S. Nolte, A. Tuennermann, and F. Lederer, Appl. Phys. Lett. **90**, 241113 (2007).
[26] F. Dreisow, M. Heinrich, A. Szameit, S. Döring, S. Nolte, A. Tünnermann, S. Fahr, and F. Lederer, Opt. Express **16**, 3474 (2008).